SUPPLEMENTARY INFORMATION

TABLE S1: Comparisons of the interplanar distance d, which was calculated using Equation: $a^2 = d_{hkl}^2[h^2 + k^2 + l^2]$, and the relative intensity of the associate peak, with other reported data from similar structures. These comparisons were used to confirm the structure of the γ-Ag_2WO_4 phase. There are some reported weak (w) and very weak (vw) reflections that were absent in our diffraction patterns.

Interplanar spacing, d (Å)				Intensity
[27]	[32]	[33]	This work	
5.401	5.35			w
				vw
	4.04	4.08		w
	3.78	3.80		w
	3.48	3.49		vw
3.308		3.28	3.29	s
		3.14		vw
	3.08		3.06	vw
	2.96	2.96	2.95	m-w
2.820	2.85	2.85	2.81	vs
	2.73	2.72		m
2.699	2.63	2.65	2.69	w
	2.42	2.44		vw
2.338		2.37	2.33	vw
	2.16	2.20		vw
	2.01	2.01	2.02	s-m-w
		1.96		w
1.909			1.906	m
1.800			1.79	m-w
			1.72	w-vw
	1.68			w
1.653	1.66		1.65	m
	1.61			w
1.478			1.47	w
1.426			1.425	w
1.410			1.409	w
1.250			1.25	w
1.217			1.217	w

Non-symmetric slab models constructed for the (100), (110) and (111) surfaces are presented in Fig S1, with thickness of 9.3 Å, 8.4 Å and 10.6 Å, respectively. The (100) and (110) surfaces were AgO_2-terminated, while the (111) surface was O_2-terminated and showed exposed Ag atoms coordinated to five O atoms, instead of four (as in the previous surfaces). On the other hand, it is important to note that the surfaces were not symmetric, and the down part of the surface (111), exposed to the vacuum, was quite different from the others. This helps explain the stability order of the surfaces: the (111) surface termination contains the most number of uncoordinated W and Ag atoms (relative to the bulk coordination), followed by the (110) surface, and lastly by the (100) surface.
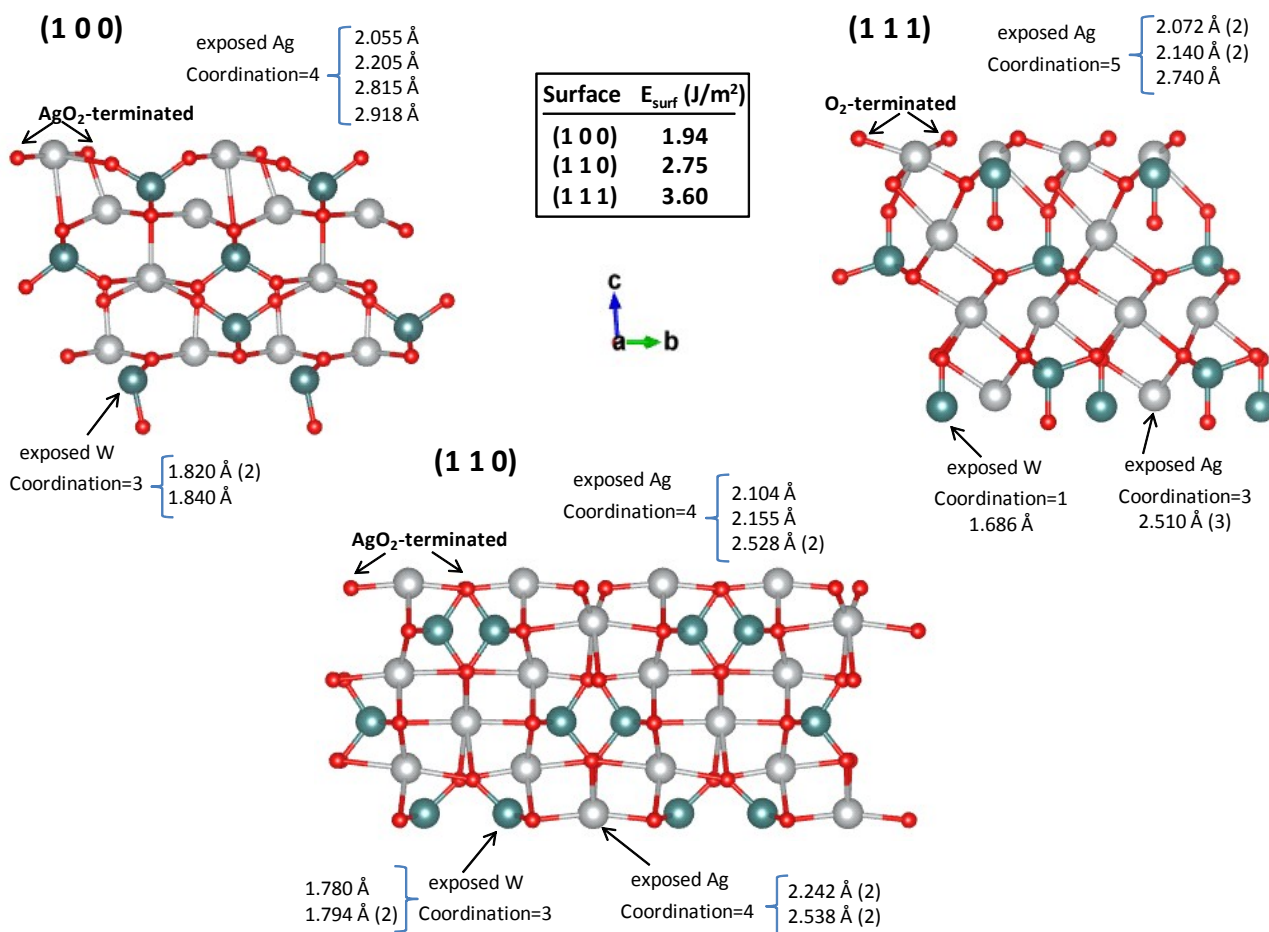

Surface	E_{surf} (J/m²)
(1 0 0)	1.94
(1 1 0)	2.75
(1 1 1)	3.60

FIG S1 Slab models constructed for (a) (100), (b) (110) and (c) (111) surfaces.

TABLE S2. Raman active modes (cm^{-1}) for the theoretical ordered and disordered γ-Ag$_2$WO$_4$ structures. The experimental Raman modes are also included for comparison purposes.

		Theoretical		Experimental
mode	Ordered	mode	Disordered	
F$_{2g}$	67.87	B$_1$, A$_1$, B$_2$	67.43, 67.58, 67.61	-
E$_g$	306.00	A$_1$, B$_1$	271.95, 293.34	283
		A$_2$, A$_1$	303.69, 307.71	
F$_{2g}$	379.43	B$_2$, A$_1$, A$_2$	366.87, 368.65, 378.92	342
		B$_1$, A$_1$	388.37, 388.87	361
-	-	B$_2$, A$_1$	589.51, 651.14	530, 658
F$_{2g}$	671.87	B$_1$, B$_2$, A$_1$	686.77, 689.39, 692.88	745
-	-	B$_1$	779.16	768
A$_g$	904.87	A$_1$	899.94	853, 880
-	-	A$_1$	936.83	912

The Kubelka-Munk method.

This methodology is used to estimate, with good accuracy, the optical band gap, E$_{gap}$, values from the UV-Vis spectra, and is based on the transformation of diffuse reflectance measurements. The Kubelka-Munk method is particularly useful within the limits of (i) assumptions when modeling in three dimensions, and (ii) an infinitely thick sample layer. The Kubelka–Munk equation is described as:

$$\frac{k}{s} = \frac{(1 - R_\infty)^2}{2R_\infty} = F(R_\infty)$$

where $F(R_\infty)$ is the Kubelka–Munk function, or absolute reflectance, of the sample; R is the reflectance when the sample is infinitely thick, $R_\infty = R_{sample}/R_{MgO}$ (R_{MgO} is the magnesium oxide (MgO) reflectance which was the standard sample used in the reflectance measurements); k is the molar absorption coefficient; and s is the scattering coefficient.

The E_{gap} and absorption coefficient of the semiconductor oxides was calculated assuming a parabolic band structure, which is described by Equation (1) in the text.

Finally, combining the Kubelka–Munk equation with Equation (1), and with the terms $k = 2\alpha$ and B ($=2A/s$) as proportionality constants, we obtained the modified Kubelka–Munk equation:

$$\left[F(R_\infty) \cdot h\nu\right]^{1/n} = B(h\nu - E_{gap})$$

Therefore, the E_{gap} values were determined by plotting a graph of $[F(R_\infty)h\nu]^{1/n}$ against $h\nu$.